Eur. J. Mineral.
2018, **30**, 1155–1162
Published online 7 September 2018

Hyršlite, $Pb_8As_{10}Sb_6S_{32}$, a new N = 3;3 member of the sartorite homologous series from the Uchucchacua polymetallic deposit, Peru

Frank N. KEUTSCH[1,*], Dan TOPA[2] and Emil MAKOVICKY[3]

[1]Harvard John A. Paulson School of Engineering and Applied Sciences and Department of Chemistry and Chemical Biology, Harvard University, 12 Oxford Street, Cambridge, MA 02138, USA
*Corresponding author, e-mail: keutsch@seas.harvard.edu
[2]Naturhistorisches Museum Wien, Burgring 7, 1010 Wien, Austria
[3]Department of Geoscience and Resource Management, University of Copenhagen, Østervoldgade 10, 1350 Copenhagen K, Denmark

Abstract: Hyršlite, $Pb_8As_{10}Sb_6S_{32}$, is a new member of the sartorite homologous series of Pb–(As,Sb) sulfosalts. It occurs in the Uchucchacua polymetallic deposit, Oyon district, Catajambo, Lima Department, Peru. Compositionally it lies between guettardite and twinnite on the one hand, and hendekasartorite on the other hand. Hyršlite is grey, opaque with metallic lustre. It is brittle, without observable cleavage or parting. Mohs hardness is derived as 4, based on VHN_{25} range of microhardness (202–221, mean 215 kg mm^{-2}). Density (calc.) = 5.26 g cm^{-3} using a simplified chemical formula. Reflectance percentages (R_{min} and R_{max}) for the four standard COM wavelengths are 32.6, 39.0 (470 nm), 32.1, 38.5 (546 nm), 31.5, 37.9 (589 nm), and 30.7, 36.7 (650 nm), respectively. The formula based on 32 S atoms per formula unit (*apfu*) is $Pb_{7.90}Sb_{5.98}As_{10.00}S_{32}$. The unit cell of hyršlite was refined from single-crystal data, with monoclinic symmetry, space group $P2_1$ a = 8.475(3) Å, b = 7.917(3) Å, c = 20.039(8) Å, β = 102.070(6)°, V = 1314.8(9) Å^3. The crystal structure of hyršlite contains 12 independent cation and 16 distinct sulfur sites. There are four fully occupied Pb sites, two fully occupied As sites, one Sb site and five mixed (As,Sb) sites. In projection parallel to the 8.5 Å axis, the crystal structure is a typical member of the sartorite homologous series, a sartorite homologue N = 3;3, and homeotype of twinnite and guettardite. Opposing surfaces of the tightly bonded double-layer in the (As,Sb)-rich slabs of the structure have different cation configurations – one resembles coordinations observed in guettardite but the opposite one, with (As,Sb) cation pairs and single polyhedra, appears unique among sartorite homologues.

Key-words: hyršlite; new mineral; sartorite homologue; Pb–(As,Sb) sulfosalt; Uchucchacua deposit; crystal structure.

1. Introduction

Members of the sartorite homologous series are Pb–As–(Sb)–(Ag, Tl) sulfosalts known from hydrothermal and low-grade metamorphic mineral deposits in which the mentioned cations form the principal ore constituents. Their structures are determined by a combination of (mostly) tricapped trigonal coordination prisms of Pb (Tl) and As (Sb) coordination pyramids in which the latter cations have well expressed lone-electron-pair character. Arsenic and antimony coordination polyhedra are in most cases interconnected by sharing common sulfur atoms and form crankshaft chains of different length and configuration (Makovicky *et al*., 2012; Makovicky & Topa, 2012; Topa *et al*., 2017; Makovicky *et al*., 2018).

For the compositional array of lowermost known homologues (so called N = 3;3 homologues with three cation sites to consider in the 4.2 Å substructure), the structures based on the presence of arsenic (practically without Sb) and variable amounts of Tl display a complex sequence of simple crankshaft chains, together with a complex W-shaped chain, and As_2S_4 and AsS_3 groups. This is the case in an anion-omission series of hepta-, ennea-, and hendekasartorite, which contain Tl as an essential constituent (Topa *et al*., 2017; Makovicky *et al*., 2018). The cases with substantial amounts of both As and Sb, such as guettardite ($Pb_{0.96}Sb_{0.99}As_{1.04}S_{4.01}$; Makovicky *et al*., 2012) and twinnite ($Pb_{0.8}Tl_{0.1}Sb_{1.3}As_{0.8}S_{4.0}$; Makovicky & Topa, 2012) have the crankshaft chains modified in order to fit the requirements of antimony which selectively substitutes for As in some positions. The discovery and structure refinement of hyršlite with the As:Sb ratio close to 5:3 shows that the variation of structural motifs built by covalent bonds of As and Sb goes even further than the two above mentioned types. Its unique bond configuration and polyhedron aggregation shows that it is not just a composition point in a solid solution series, and justifies its existence as an independent mineral species.

The name is for the Dr. Jaroslav Hyršl, Czech mineralogist and expert on Peruvian minerals, in particular on the

0935-1221/18/0030-2797 $ 3.60
https://doi.org/10.1127/ejm/2018/0030-2797

Uchucchacua deposit. English pronunciation is Hirshl (as in "*h*e", "*gi*ve" and "*sh*e"). The mineral and its name were approved by the Commission for New Minerals and Mineral Names under the number 2016-097. The holotype is deposited in the reference collection of the Naturhistorisches Museum Wien, catalogue number O 201.

2. Occurrence

The mineral occurs in the Uchucchacua polymetallic deposit, Oyon district, Catajambo, Lima Department, Peru. Uchucchacua is an Ag–Mn–Pb–Zn vein, replacement and skarn mineral deposit in the central Andes of Peru, hosted by limestones (Bussell *et al.*, 1990). The Uchucchacua deposit is surrounded by andesitic and dacitic volcanic deposits and intrusions of Late Oligocene age (approximately 25 Ma) and its formation might be connected with them (Bissig *et al.*, 2008). Ores were generated as fissure infill and replacement of adjacent limestone in a succession of antiforms and synforms. In the first stage, silicates of Mn, Fe and Ca (rhodonite, bustamite, *etc.*) were deposited. In Stage 2, friedelite, magnetite, and an array of common sulfides were deposited, including Fe-rich sphalerite, manganoan wurtzite and alabandite, with pyrrhotite unstable. Main gangue minerals were calcite, kutnohorite, rhodochrosite, and quartz. In the late Stage 3, Ag, As, and Sb were introduced, forming sulfosalts. In this stage, Fe-poor sphalerite and alabandite coexist with calcite and pyrite, indicating an increase in sulfur fugacity and decrease in temperature. Bussell *et al.* (1990) ascribe orpiment, marcasite and siderite to a supergene stage, together with Mn oxides, goethite and cerussite. This deposit was a source of benavidesite (Leone *et al.*, 2003), uchucchacuaite ($AgMnPb_3Sb_5S_{12}$, Moëlo *et al.*, 1984), and the Socorro section, which was rich in alabandite and in which the samples with hyršlite were found, was the source of menchettiite ($AgPb_{2.40}Mn_{1.60}Sb_3As_2S_{12}$; Bindi *et al.*, 2012), manganoquadratite ($AgMnAsS_3$; Bonazzi *et al.*, 2012), keutschite, (Cu_2AgAsS_4; Topa *et al.*, 2014), agmantinite (Ag_2MnSnS_4; Keutsch *et al.*, 2015), and spryite ($Ag_8(As^{3+}, As^{5+})S_6$; Bindi *et al.*, 2017).

Hyršlite was found in the sample in which menchettiite was described in association with orpiment. It was given to one of the authors (F.N.K.) by the mineral dealer John Veevaert. Subsequently, it was found in two additional samples supplied by one of the authors (F.N.K.) which contain orpiment and Pb–Ag–Mn–Sb–As–S sulfosalts. The mineral occurs in close association with orpiment, quartz, tennantite/tetrahedrite, menchettiite and manganoquadratite in a calcite matrix.

3. Appearance and physical properties

Hyršlite occurs as very rare individual crystals (Fig. 1), closely associated with orpiment, manganoquadratite, stibnite and Pb–Ag–Mn–Sb–As–S sulfosalts, and as euhedral-to-anhedral grains intergrown with manganoquadratite and Pb–Ag–Mn–Sb–As–S sulfosalts, including menchettiite.

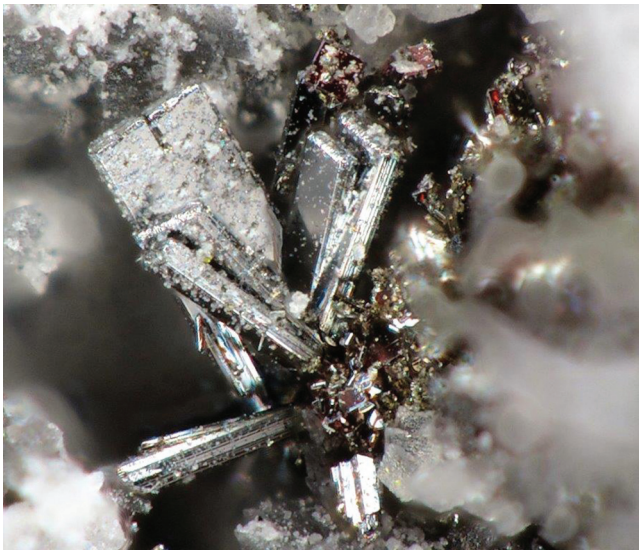

Fig. 1. Hyršlite crystals to about 300 μm associated with smaller, quadratic, red manganoquadratite crystals. Photo by Christian Rewitzer. (online version in colour).

In Fig. 2, hyršlite appears to be partially replaced by this association. The maximum crystal size of hyršlite is about 300 μm.

Hyršlite is grey, with metallic lustre. It is opaque and non-fluorescent. Streak is black. The mineral is brittle, without observable cleavage or parting; fracture is conchoidal. A Mohs hardness of 4 is derived on the basis of VHN_{25} results: the range of microhardness values is 202–221, mean 215 kg mm^{-2} (mean of 10 measurements). Density could not be measured because of paucity of available material. Density (calc.) = 5.26 g cm^{-3} using the simplified chemical formula.

3.1. Optical properties

In reflected light, hyršlite is greyish-white, with red internal reflections on thin edges or at grain boundaries. Pleochroism was not detected, bireflectance is moderate. Anisotropism is distinct in dark grey-to-creamy rotation tints. Reflectance values (WTiC standard in air) are given in Table 1. At short wavelengths, the reflectance values are lower than those of hepta- to hendekasartorites (Topa *et al.*, 2017) but the decrease in the *R* values towards the long wavelengths of visible light is more moderate than for the "sartorite" species (Fig. 3).

3.2. Chemical data

Chemical analyses (11 points on 3 grains) were carried out using a JEOL Hyperprobe JXA-8530F (wavelength-dispersive mode, 25 kV, 20 nA, 2 μm beam diameter, ZAF correction procedure) electron microprobe. No other elements than those indicated in Table 2 were detected.

The empirical formula (based on 56 *apfu*, 24 Me + 32 S) is $Pb_{7.92}Sb_{6.00}As_{10.02}S_{32.06}$. (ΣMe = 23.94).

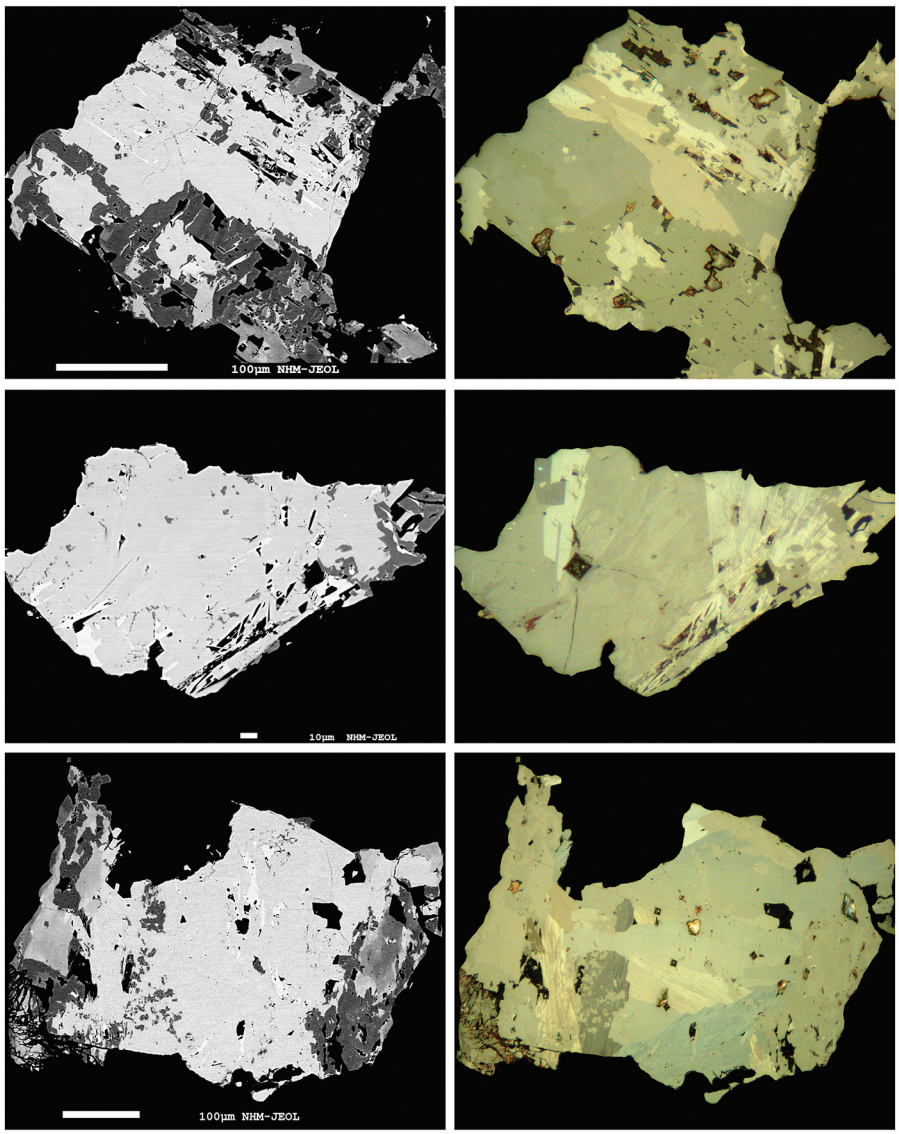

Fig. 2. Euhedral-to-anhedral hyršlite grains intergrown with manganoquadratite and Pb–Ag–Mn–Sb–As–S sulfosalts, including menchettiite. The left-side pictures are back-scattered electron (BSE) images, those on the right are the corresponding reflected-light images (crossed polarizers). The aggregates contain a grey central hyršlite grain associated with menchettiite (dark) and other Pb–Ag–Mn–Sb–As–S sulfosalts. (online version in colour).

The formula based on 32 S *apfu* is $Pb_{7.90}Sb_{5.98}As_{10.00}S_{32}$. (ΣMe = 23.89) and the empirical formula based on 24 Me *apfu* is $Pb_{7.94}Sb_{6.01}As_{10.05}S_{32.15}$. (ΣMe = 24). The crystal-structure formula is $Pb_8Sb_6As_{10}S_{32}$. The simplified formula is $Pb_8Sb_6As_{10}S_{32}$. Refinement of the structure with several mixed sites is in a good agreement with the chemical analyses, performed with Pb$M\alpha$ and As$L\alpha$ as measured lines.

3.3. Crystallography and crystal structure

The unit cell of hyršlite was refined from single-crystal data as a = 8.475(3) Å, b = 7.917(3) Å, c = 20.039(8) Å, β = 102.070(6)°, V = 1314.8(9) Å^3, monoclinic symmetry, space group $P2_1$. The unit-cell dimensions are similar to those of guettardite, $PbAsSbS_4$ (a = 8.527(4) Å, b = 7.971(4) Å, c = 20.102(10) Å, β = 101.814(7)°, which has a higher Sb/As ratio resulting in a slightly larger unit-cell volume (1337.4 Å^3), but the space group of guettardite (Makovicky *et al.*, 2012) is $P2_1/c$, heralding important structure differences. Hyršlite occurs as euhedral grains and free-standing crystals. Crystal forms and twinning are not morphologically observable. The a:b:c ratio calculated from the unit-cell parameters is 1.057:1:3.091.

Several fragments of hyršlite were tested and a fragment with irregular shape and 0.02 × 0.04 × 0.07 mm in size was found to be suitable for data collection on a Bruker AXS three-circle diffractometer equipped with a CCD area detector. The SMART (Bruker AXS, 1998a) system of programs was used for unit-cell determination and data

Table 1. Reflectance values (%) for hyršlite in air (WTiC standard).

λ (nm)	R_{min}	R_{max}	λ (nm)	R_{min}	R_{max}
400	33.6	39.0	560	31.8	38.3
420	32.3	38.8	580	31.8	38.1
440	32.6	38.9	**589**	**31.5**	**37.9**
460	32.6	39.1	600	31.4	37.8
470	**32.6**	**39.0**	620	31.2	37.4
480	32.4	39.0	640	30.9	37.0
500	32.6	39.1	**650**	**30.7**	**36.7**
520	32.4	38.9	660	30.6	36.3
540	32.2	38.6	680	30.0	35.7
546	**32.1**	**38.5**	700	29.7	35.5

Note: The reference wavelengths required by the Commission on Ore Mineralogy (COM) are given in bold.

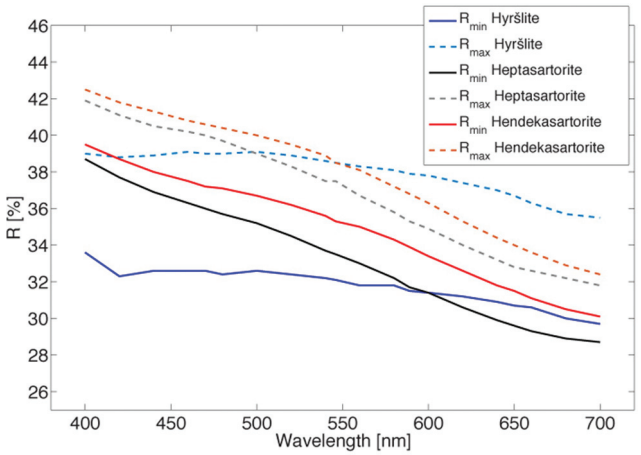

Fig. 3. Reflectance curves of hyršlite compared with those of heptasartorite and hendekasartorite. (online version in colour).

Table 2. Chemical analytical data (wt%) for hyršlite.

	Mean (*SD*)	Range (min–max)	Standard and line
Pb	39.26 (31)	38.72–39.71	Galena (nat.) Pb *Mα*
Sb	17.47 (56)	16.55–18.41	Stibnite (nat.) Sb *Lα*
As	17.97 (33)	17.28–18.46	Lorandite (nat.) As *Lα*
S	24.60 (13)	24.40–24.75	Lorandite (nat.) S *Kα*
Total	99.30 (43)	98.55–100.27	

The empirical formula (based on 56 *apfu*, 24 Me + 32 S) is $Pb_{7.92}Sb_{6.00}As_{10.02}S_{32.06}$ (ΣMe = 23.94). The empirical formula (based on 32 S *apfu*) is $Pb_{7.90}Sb_{5.98}As_{10.00}S_{32}$. (ΣMe = 23.89). The empirical formula (based on 24 Me *apfu*) is $Pb_{7.94}Sb_{6.01}As_{10.05}S_{32.15}$. (ΣMe = 24).

collection, SAINT+ (Bruker AXS, 1998b) for the reduction of the intensity data, and XPREP (Bruker AXS, 1997) for space-group determination and empirical absorption correction based on pseudo ψ-scans. The noncentrosymmetric space group $P2_1$ proposed by the XPREP program was chosen in conformity with the monoclinic symmetry of the lattice and intensity statistics. The structure of hyršlite was solved by direct methods (Sheldrick, 2008), which revealed

Table 3. Crystal data and summary of parameters describing data collection and refinement for hyršlite.

Crystal data	
Chemical formula	$Pb_8As_{10}Sb_6S_{32}$
Formula weight	4158.5
Crystal system	monoclinic
Space group	$P2_1$ (no. 4)
D_x (g cm^{-3})	5.26
Reflections for cell parameter	2525
Unit-cell parameters	
a (Å)	8.475(3)
b (Å)	7.917(3)
c (Å)	20.039(8)
β (°)	102.070(6)
V (Å^3)	1314.8(9)
Z	2
μ (mm^{-1})	36.1
Crystal size (mm)	0.03 × 0.04 × 0.06
Data collection	
T_{min}, T_{max}	0.173, 0.391
Measured reflections	6769
Independent reflections	3618
Observed reflections	2862 [$I > 2\sigma(I)$]
R_{int} (%), $R_{(sigma)}$(%)	11.57, 13.29
θ_{max} (°)	23.26
Range of *h, k, l*	$-9 \le h \le 8$, $-8 \le k \le 8$, $-18 \le l \le 22$
Refinement (on F_o^2)	
$R[F_o > 4\sigma(F_o)]$	0.0728
$wR(F_o^2)$	0.1704
S (GooF)	1.164
Parameters refined	235
Weighting scheme	$a = 0.0769$, $b = 28.2$
$w = 1/[\sigma^2(F_o^2)+(aP)^2+bP]$	where $P = (F_o^2+2F_c^2)/3$
$(\Delta/\sigma)_{max}$	0.002
$\Delta\rho_{max}$ (e/Å^3)	3.24 (0.62 Å from S15)
$\Delta\rho_{min}$ (e/Å^3)	−2.26 (0.95 Å from Pb4)
Atomic scattering factors	International Tables for X-Ray Crystallography, Vol. C (1992) (Tables 4.2.6.8 and 6.1.1.4)

most of the atom positions. In subsequent cycles of the refinement (Sheldrick, 2008), remaining atom positions were deduced from difference Fourier syntheses by selecting from among the strongest maxima at appropriate distances. The resulting R_1 is 0.0728 for 2862 reflections with $Fo > 4\sigma(Fo)$ and 0.0932 for all 3618 data. Crystal data and summary of parameters describing data collection and refinement are presented in Table 3, coordinates, occupancy factors and displacement parameters of atoms in Table 4, and selected interatomic distances (Å) in Table 5.

Powder X-ray data were not collected, due to the small size of the crystals and admixture with other sulfosalts, but were calculated on the basis of the results of the single-crystal structure determination. Data are listed in Table S1, freely available online (along with the CIF file) as Supplementary Material linked to this article on the GSW website of the journal: https://pubs.geoscienceworld.org/eurjmin).

The crystal structure of hyršlite contains 12 independent cation and 16 distinct sulfur sites. There are four fully

Table 4. Coordinates, occupancy factors and displacement parameters (Å^2) of atoms in hyršlite.

Atom	Label	sof	*x*	*y*	*z*	*U*eq/iso
Pb1	Pb		0.4775(3)	0.3171(3)	0.45203(13)	0.0410(8)
Pb2	Pb		0.0303(4)	0.1393(4)	0.05166(15)	0.0514(9)
Pb3	Pb		0.5213(4)	0.1390(4)	0.05165(15)	0.0514(10)
Pb4	Pb		0.9732(4)	0.3145(4)	0.44465(16)	0.0579(10)
As5	As		0.8058(6)	0.7355(8)	0.1147(2)	0.0180(12)
As6	As		0.3688(6)	0.0550(7)	0.2405(2)	0.0153(11)
Sb7	Sb		0.8920(6)	0.0247(5)	0.2776(2)	0.0407(13)
As8	As,Sb	0.84(5), 0.15	0.6609(8)	0.7335(8)	0.3727(3)	0.040(2)
Me9	*As,Sb*	*0.53(5), 0.47*	0.0875(7)	0.4139(8)	0.2342(4)	0.063(3)
Sb10	Sb,As	0.82(5), 0.18	0.3205(8)	0.7072(6)	0.1383(2)	0.059(2)
As11	As,Sb	0.87(5), 0.13	0.2057(8)	0.7316(8)	0.3733(3)	0.045(2)
Me12	*As,Sb*	*0.59(5), 0.41*	0.6470(7)	0.4118(8)	0.2358(4)	0.064(3)
S1	S		0.1312(16)	0.1969(18)	0.3328(6)	0.024(3)
S2	S		0.7597(18)	0.8819(18)	0.0165(8)	0.028(4)
S3	S		0.5447(14)	0.9009(16)	0.1972(7)	0.026(3)
S4	S		0.7008(16)	0.1979(19)	0.3326(6)	0.024(3)
S5	S		0.1507(15)	0.8976(15)	0.1972(7)	0.026(3)
S6	S		0.2681(18)	0.8579(16)	0.0344(7)	0.022(3)
S7	S		0.8382(18)	0.2258(15)	0.1758(6)	0.023(3)
S8	S		0.4031(13)	0.0629(13)	−0.0921(5)	0.008(2)
S9	S		0.735(2)	0.570(2)	0.4753(8)	0.035(4)
S10	S		0.246(2)	0.569(2)	0.4759(8)	0.034(4)
S11	S		0.962(3)	0.904(3)	0.4107(13)	0.079(7)
S12	S		0.994(1)	0.562(1)	0.0923(5)	0.008(2)
S13	S		0.449(2)	0.901(2)	0.4051(9)	0.045(4)
S14	S		0.329(3)	0.270(3)	0.1647(10)	0.061(6)
S15	S		0.4109(3)	0.527(3)	0.3117(11)	0.074(6)
S16	S		0.892(4)	0.574(4)	0.2929(14)	0.094(9)

occupied Pb sites, two fully occupied As sites, one Sb site and five mixed (As,Sb) sites (see Table 4). In the projection along [100], the structure is a typical structure of the $N = 3$ member of the sartorite homologous series. There are four crystallographically distinct tricapped trigonal prismatic sites of Pb combined into zig-zagging "walls" which separate As–Sb based slabs of the structure (Fig. 4). The slabs are composed of tightly bonded double ribbons with the two ribbon surfaces denoted as layers L1 and L2 (Fig. 4) which, unlike those in guettardite and twinnite, are differently configured. The surface layer L2, with Sb7, As5, As6 and a mixed position Sb10 (Fig. 5a) resembles such a surface in guettardite, but the Sb10 position ($Sb_{0.82}As_{0.18}$) in the group As5–Sb10–As6 of layer L1, is symmetrical, whereas in guettardite it was an asymmetrically flipping position with two opposing 2.70 Å bond distances. Here we have a tightly bonded pair Sb10–As6 instead of the rudimentary three-member chain that we have seen in guettardite. The term "tightly bonded" means here 'bonded via short strong Me–S bonds to two common S atoms'.

The opposing ribbon surface, denoted as layer L1 (Fig. 5b), contains tightly bonded mixed-occupancy Sb–As pairs Me9–Me12, with Sb occupancies equal to 0.53 and 0.59, respectively, and with bond lengths in full agreement with the half-half occupancies observed. An uninterrupted periodic sequence of slightly mixed sites As8–As11 occupies a margin of this ribbon surface, with As occupancies equal to 0.84 and 0.87, respectively. Both sites exhibit a trend to flip towards S15 (Table 5), situated between the Me9–Me12 pairs and bonded to Pb1.

Across the inter-ribbon space, the two-cation groups of one ribbon face match nicely with the marginal groups on the opposite face, anions always matching the opposing cations.

The change of configuration from that in guettardite (which contains a diagonal 3D crankshaft chain of 8 cation sites, which has its 2D halves respectively situated on the front and back surfaces of the double-ribbon interconnected by an inversion-related pair of Sb pyramids in the ribbon centreline) to that in hyršlite (which has a half-open Sb7–Me9–Me12 cage spanning both surfaces of the ribbon (Fig. 6); this cage is isolated from As8 to As11, and As6 to Sb10 configurations) results from *bond orientations* of Me9 and Me12 in hyršlite *different* from those of the corresponding sites in guettardite. This difference is connected to a more pronounced separation of As and Sb in these sites in guettardite. The only obvious agent of change in the fundamental structure principles of this structure based on covalent bonds is the pronounced change in the As/Sb ratio from guettardite to hyršlite.

The symmetric organization of the As5–As6–Sb7–Sb10 surface in hyršlite (layer L2) is fully reproduced in pierrotite (Engel *et al*., 1983). The cation pair is asymmetric again, as Sb3–As4 in pierrotite, the here asymmetric As5–Sb7 configurations are present as symmetric As1 and As3 in pierrotite. The opposite face in pierrotite is differently configured, it is

Table 5. Selected interatomic distances (Å) in hyršlite.

Pb1–		Pb2–		Pb3–		Pb4–	
S13	2.877(18)	S12	2.914(10)	S8	2.908(10)	S11	2.92(3)
S10	2.907(18)	S2	3.039(15)	S2	3.053(15)	S1	2.991(12)
S9	2.923(18)	S6	3.071(14)	S6	3.060(15)	S9	3.010(17)
S10	3.165(17)	S2	3.120(15)	S2	3.142(14)	S4	3.009(13)
S15	3.210(17)	S14	3.200(15)	S14	3.230(15)	S10	3.033(17)
S9	3.207(17)	S6	3.247(15)	S6	3.233(15)	S9	3.287(19)
S13	3.424(19)	S7	3.316(13)	S7	3.328(14)	S11	3.32(3)
S4	3.477(13)	S5	3.459(15)	S3	3.447(15)	S10	3.317(18)
S1	3.507(13)	S12	3.472(11)	S8	3.480(11)	S16	3.61(3)
As5–		As6–		Sb7–		(As,Sb)8–	
S8	2.204(12)	S3	2.235(13)	S1	2.500(14)	S9	2.400(18)
S12	2.220(12)	S5	2.247(13)	S4	2.543(14)	S13	2.43(2)
S2	2.248(17)	S14	2.26(2)	S7	2.553(11)	S15	2.76(2)
S3	3.301(13)	S1	3.207(13)	S11	2.78(3)	S11	2.84(3)
S5	3.304(13)	S4	3.230(14)	S5	3.145(13)	S16	3.05(3)
S16	3.72(3)	S13	3.449(18)	S3	3.198(12)	S3	3.690(16)
				S16	3.58(3)		
Me9–		(Sb,As)10–		(As,Sb)11–		Me12–	
S16	2.56(3)	S6	2.360(13)	S10	2.388(17)	S16	2.50(3)
S1	2.586(16)	S3	2.535(12)	S13	2.43(2)	S4	2.543(16)
S7	2.649(15)	S5	2.538(13)	S11	2.71(3)	S7	2.657(15)
S14	2.94(2)	S8	2.926(12)	S15	2.83(2)	S15	2.91(2)
S15	2.98(2)	S12	2.959(12)	S16	3.07(3)	S14	2.99(2)
S12	3.023(13)	S14	3.50(2)	S5	3.702(16)	S8	3.064(13)
		S15	3.69(2)	S1	3.796(16)		

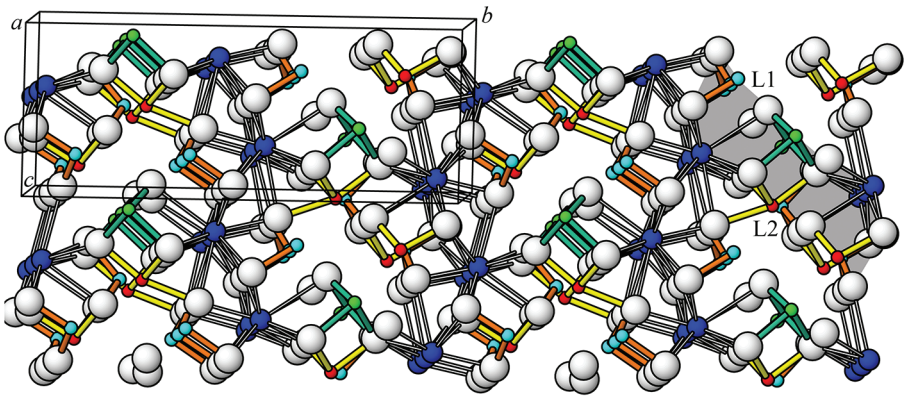

Fig. 4. The crystal structure of hyršlite viewed approx. along [100]. Colour coding: blue – lead, cyan – full As sites, red – full Sb sites, green – half-half (As,Sb) mixed sites. Four crystallographically distinct tricapped trigonal prismatic sites of Pb combined into zig-zagging "walls" separate As-Sb based slabs of the structure. A tightly bonded double ribbon with configurationally different SnS-like surfaces (L1 and L2) is indicated in grey. The layers L1 and L2 are asymmetrical and have different chemistry. (online version in colour).

Sb-rich (as opposed to the just described "As-enriched" face) and it copies the chain pattern in twinnite.

Local reflection planes perpendicular to (100) are a prominent feature of Figs. 5a and 5b. In the projection on (010), the structure displays 2_1 screw axes positioned in the zig-zag [010] arrays of Pb atoms and the series of slightly approximate mirror planes perpendicular to [100] is spaced at 1/4 *a* and 3/4 *a* on the *a* axis. This becomes 3/4 *a* and 1/4 *a* when one [001] *c* period has been passed. These planes of symmetry reflect the unit cell into its "conjugate".

These reflection planes are violated only by the slight asymmetry of the As8 and As11 bonds and the small Me12–Me9 occupational difference. These small configurational and compositional differences, expressed by the just described mirror planes, are parallel to, and partly connected with, the statistical occupancy of cation sites, especially that of the Me9–Me12 pair. They explain the near 50:50 merohedral twinning indicated by the refinement and backed by the finely lamellar character of some of the hyršlite crystal bundles. Should the situation be characterized as a disorder or as detailed twinning? We find the situation close to the microcline–orthoclase conundrum in its nature.

A remarkable fact is that the cation and anion sites in hyršlite correspond topologically to those in guettardite but they have a different organization of short bonds and longer interatomic distances, *resulting in a different structure.*

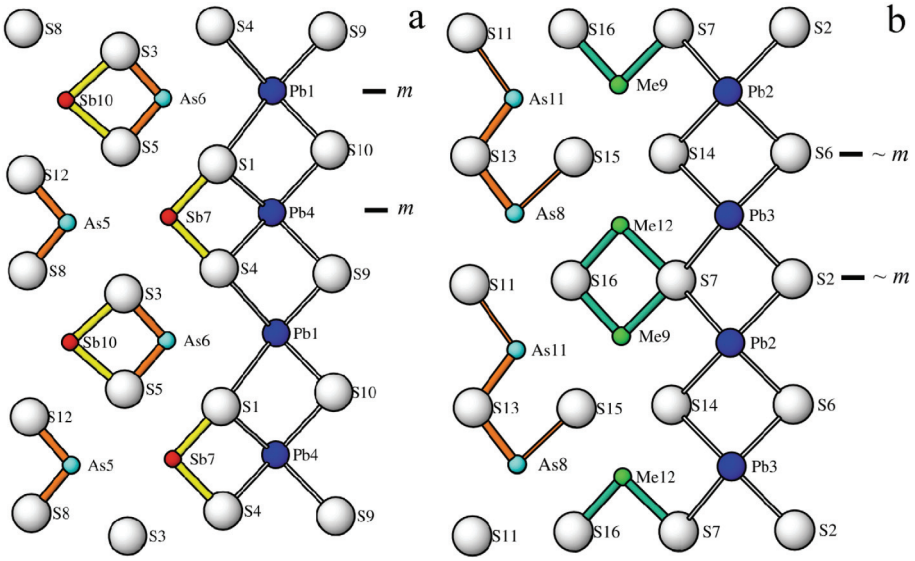

Fig. 5. The opposing surfaces (layer L2 (a) and layer L1 (b)) of the double-ribbon in hyršlite. Two unit-cells of hyršlite along *a* axis are illustrated, showing the periodic sequences of sites occupied by As, Sb and Pb and the orientation and length of cation-sulfur bonds. Colour coding as in Fig. 4. The *approximate* (100) reflection planes are indicated; see text for details. (online version in colour).

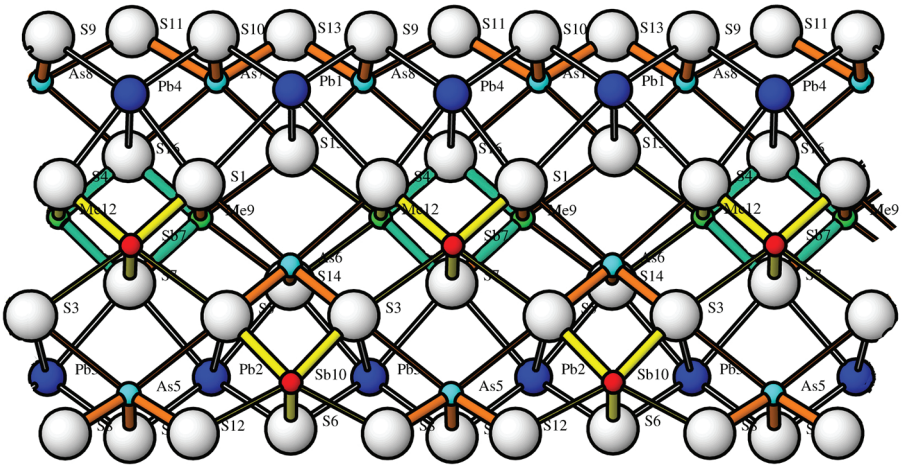

Fig. 6. The double-ribbon of hyršlite. The *a* axis is horizontal. Colour coding as in Fig. 4. (online version in colour).

Table 6. Comparative data for hyršlite and related sartorite homologues with $N = 3$.

Mineral	Hyršlite	Guettardite	Twinnite
Formula	$Pb_8As_{10}Sb_6S_{32}$	$Pb_8As_8Sb_8S_{32}$	$Pb_{6.4}Tl_{0.8}Sb_{10.4}As_{6.4}S_{32}$
Crystal system	Monoclinic	Monoclinic	Monoclinic
Space group	$P2_1$	$P2_1/c$	$P2_1/n$
Cell parameters			
a (Å)	8.475(3)	8.527(4)	7.997(2)
b (Å)	7.917(3)	7.971(4)	19.517(5)
c (Å)	20.039(8)	20.102(10)	8.634(2)
β (°)	102.070(6)	101.814(7)	91.061(4)
V (Å^3)	1314.8(9)	1337.3(11)	1347.4(6)
Z	1	1	1
Reference*	1	2	3

*1 – this study; 2 – Makovicky *et al.* (2012); 3 – Makovicky & Topa (2012).

Coordination pyramids of As and Sb have strongly trapezoidal bases. With the exception of the asymmetric bonding scheme of As11 and As8, all coordinations in the pyramidal base may be taken as mirror-symmetrical. The only pseudo-octahedral coordination is that of Sb7, with the under-base distance of 2.75 Å indicating a partly flipping character of the bonds, alternatively to the pyramidal vertex and to the pyramidal "antivertex".

Augmented displacement factors distinguish Pb4 (neighbour to As8, Me9, and Me12), Sb7 (flipping out of pyramid base), Sb10/As10, As9/Sb9, and Sb12/As12. The three latter ones reflect the As/Sb substitution in nearly the same spots of the coordination polyhedron but slightly displaced against one another because of different bond-to-opposing distance ratios.

4. Conclusion

Hyršlite is a new member of the sartorite homologous series (Makovicky, 1985; Makovicky & Topa, 2015) with $N_{1,2}$ = 3;3 *i.e.* = 3. The unit cell of hyršlite, $Pb_8As_{10}Sb_6S_{32}$, is similar to that of guettardite, $Pb_8As_8Sb_8S_{32}$, but the space group of the former is $P2_1$ and that of the latter is $P2_1/c$, heralding the observed important structure differences (Table 6).

Hyršlite is a splendid example of the importance of cation ratios in covalent compounds, even when they involve ratios of crystal-chemically related elements with quantitative rather than qualitative differences in bonding/electron configuration properties (covalent radius, lone electron pair eccentricity, sometimes electronegativity). In this case, it is a rather unique configuration of conjugated As and Sb coordination pyramids in the surfaces of tightly bonded double-ribbons, which is situated between the configurations in arsenic-based M-sartorite species (Topa *et al.*, 2017; Makovicky *et al.*, 2018) and the mixed-cation guettardite and twinnite species (Table 6).

References

Bindi, L., Keutsch, F.N., Bonazzi, P. (2012): Menchettiite, $AgPb_{2.40}Mn_{1.60}Sb_3As_2S_{12}$, a new sulfosalt belonging to the lillianite series from the Uchucchacua polymetallic deposit, Lima Department, Peru. *Am. Mineral.*, **97**, 440–446.

Bindi, L., Keutsch, F.N., Morana, M., Zaccarini, F (2017): Spryite $Ag_8(As^{3+}_{0.5}As^{5+}_{0.5})S_6$: structure determination and inferred absence of superionic conduction of the first As^{3+}-bearing argyrodite. *Phys. Chem. Minerals*, **44**, 75–82.

Bissig, T., Ulrich, T.D., Tosdal, R.M., Friedman, R., Ebert, S. (2008): The space-time distribution of Eocene to Miocene magmatism in the central Peruvian polymetallic province and its metallogenetic implications. *J. South Am. Earth Sci.*, **26**, 16–35.

Bonazzi, P., Keutsch, F.N., Bindi, L. (2012): Manganoquadratite, $AgMnAsS_3$, a new manganese-bearing sulfosalt from the Uchucchacua polymetallic deposit, Lima Department, Peru: Description and crystal structure. *Am. Mineral.*, **97**, 1199–1205.

Bussell, M.A., Alpers, C.N., Petersen, U., Shepherd, T.J., Bermudez, C., Baxter, A.N. (1990): The Ag-Mn-Pb-Zn vein, replacement, and skarn deposits of Uchucchacua, Peru – studies of structure, mineralogy, metal zoning, Sr isotopes, and fluid inclusions. *Econ. Geol.*, **85**, 1348–1383.

Bruker AXS (1997): XPREP, Version 5.1, Bruker AXS Inc, Madison, USA.

Bruker AXS (1998a): SMART, Version 5.0, Bruker AXS Inc, Madison, USA.

Bruker AXS (1998b): SAINT, Version 5.0, Bruker AXS Inc, Madison, USA.

Engel, P., Gostojic, M., Nowacki, W. (1983): The crystal structure of pierrotite, $Tl_2(Sb,As)_{10}S_{16}$. *Z. Kristallogr.*, **165**, 209–215.

Jambor, J.L. (1967a): New lead sulfantimonides from Madoc, Ontario. Part 2 – Mineral descriptions. *Can. Mineral.,* **9**, 191–213.

Jambor, J.L. (1967b): New lead sulfantimonides from Madoc, Ontario – Part 1. *Can. Mineral.*, **9**, 7–24.

Keutsch, F.N., Topa, D., Takagi-Fredrickson, R., Makovicky, E., Paar, W. (2015): Agmantinite, IMA 2014–083, CNMNC Newsletter 23. *Mineral. Mag.*, **79**, 57.

Kraus, W. & Nolze, G. (1999): PowderCell 2.3, Federal Institute for Materials Research and Testing, Berlin.

Leone, P., Le Leuch, L.M., Palvadeau, P., Molinie, P., Moëlo, Y. (2003): Single crystal structures and magnetic properties of two iron or manganese-lead-antimony sulfides: $MPb_4Sb_6S_{14}$ (M: Fe, Mn). *Solid State Sci.*, **5**, 771–776.

Makovicky, E. (1985): The building principles and classification of sulphosalts based on the SnS archetype. *Fortschr. Mineral.*, **63**, 45–89.

Makovicky, E. & Topa, D. (2012): Twinnite, $Pb_{0.8}Tl_{0.1}Sb_{1.3}As_{0.80}S_4$, the OD character and the question of its polytypism. *Z. Kristallogr.*, **227**, 468–475.

Makovicky, E. & Topa, D. (2015): Crystal chemical formula for sartorite homologues. *Mineral. Mag.*, **79**, 25–31.

Makovicky, E., Topa, D., Stoeger, B. (2018): The crystal structures of heptasartorite, $Tl_7Pb_{22}As_{55}S_{108}$ and enneasartorite, $Tl_6Pb_{32}As_{70}S_{140}$, two members of an anion-omission series of complex sulfosalts. *Eur. J. Mineral.*, **30**, DOI: 10.1127/ejm/2018/0030-2797.

Makovicky, E., Topa, D., Tajjedin, H., Rastad, E., Yaghubpur, A. (2012): The crystal structure of guettardite, $PbAsSbS_4$. *Can. Mineral.*, **50**, 253–265.

Moëlo, Y., Oudin, E., Picot, P., Caye, R. (1984): Uchucchacuaite, $AgMnPb_3Sb_5S_{12}$, a new mineral of the andorite series. *Bull. Minéral.*, **107**, 597–604.

Sheldrick, G.M. (2008): A short history of *SHELX*. *Acta Crystallogr.*, **A64**, 112–122.

Topa, D., Takagi-Fredrickson, R., Stanley, C. (2014): Keutschite, IMA 2014–038, CNMNC Newsletter 21. *Mineral. Mag.*, **78**, 79–80.

Topa, D., Makovicky, E., Stoeger, B., Stanley, C.J. (2017): Heptasartorite, $Tl_7Pb_{22}As_{55}S_{108}$, enneasartorite, $Tl_6Pb_{32}As_{70}S_{140}$, and hendekasartorite, $Tl_2Pb_{48}As_{82}S_{172}$, three members of the anion-omission series of "sartorites" from the Lengenbach quarry at Binntal, Wallis, Switzerland. *Eur. J. Mineral.*, **29**, 701–712. DOI: 10.1127/ejm/2017/0029-2634.

Received 25 January 2018
Modified version received 10 May 2018
Accepted 11 May 2018